A New Approach to Flexible-Shaft Vibration Control

I. REDMOND

ABSTRACT

The ability of active magnetic bearings to influence the dynamic characteristics of rotating equipment is well documented. Present-day magnetic bearings are designed to introduce a radial (and/or axial) control force to the rotating element, the bearing dynamic parameters having been selected to minimize system vibrations. This paper describes a different control strategy which may be considered as being complementary, or in some cases an alternative, to the normal approach. In this case the control effort is introduced to the rotor in an angular sense. A theoretical study is performed and it is shown that cases exist where such an approach could be beneficial from a rotordynamics standpoint.

INTRODUCTION

Active Magnetic Bearings (AMB's) have been around for some time now and have been shown, in many instances, to offer significant advantages over their conventional passive counterparts, i.e. oil-film and rolling element bearings.

Application of the AMB is becoming more widespread as unit costs decrease and more information on user experience, in terms of performance and reliability, is made available.

Utilization of active magnetic bearings generally provides the machine designer with greater freedom in selecting the system parameters and thus greatly enhances his ability to optimize the machine dynamics in some fashion [1], whilst ensuring that equipment performance criteria can be met. Currently, magnetic bearings are employed to control rotor motion in both the radial [2] and axial [3] directions.

In this paper, an additional mode of control, termed angular control [4], will be presented and it's effectiveness, in comparison to conventional radial control, assessed analytically on a simple rotor system and on a full scale rotor.

RADIAL, AXIAL AND ANGULAR CONTROL

RADIAL CONTROL

The construction and principle of operation of present-day AMB's is well documented [5]. Radial magnetic bearings are constructed in a manner similar to that of induction machines.

Dr. Irvin Redmond, Consulting Services Dept., Saudi Aramco, Dhahran 31311, Saudi Arabia.

Fig. 1a depicts a cross-sectional view of a typical radial AMB. The device provides both a static force, to counter rotor weight, along with a dynamic component to limit rotor motion about some predetermined position.

AMB's are unstable in open-loop configuration and so displacement-related feedback control is employed to achieve the desired system dynamic characteristics, i.e.. stiffness and damping. A variety of control strategies may be employed [6].

AXIAL CONTROL

Axial AMB's operate in a similar manner. Shaft axial displacement is monitored and any rotor thrust present is countered by an axial control force applied to the rotor through a shaft-mounted disc (Fig. 1b). Axial stiffness and damping forces are provided by suitable selection of the proportional and derivative control feedback gains, respectively [3].

ANGULAR CONTROL

The proposed implementation of angular control is shown schematically in Figure 1c. Here, four horseshoe-type electromagnets are employed at each side of a high-resistivity, or laminated, shaft-mounted disc. Each magnet is located in a single quadrant of the disc. The arrangement is almost identical to that adopted for axial control. However, in this case the electromagnets are utilized to apply a control moment.

The electromagnets operate in pairs, each active pair consisting of diametrally opposed magnets, one on either side of the disc. A signal proportional to shaft slope is obtained by summing shaft displacement measurements taken at each side of the disc. This signal can then be utilized in a feedback control loop to provide the rotor system with *angular* stiffness and/or damping.

Note that in contrast to the radial and axial control schemes, angular control demands only the application of a *dynamic* force.

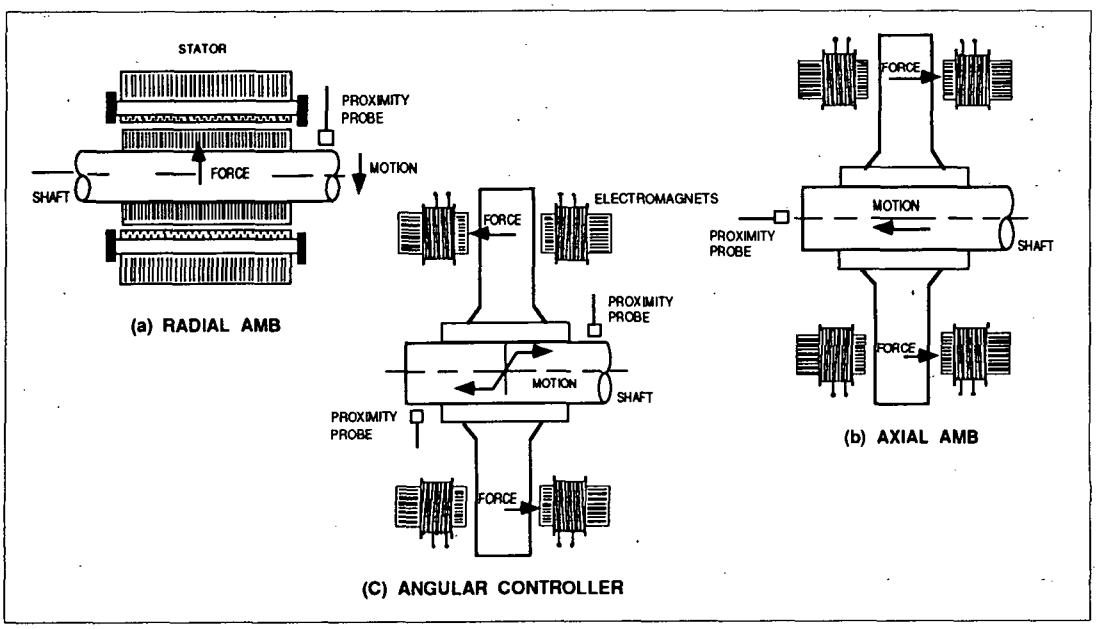

FIGURE 1. ACTIVE MAGNETIC CONTROL METHODS

WHY ANGULAR CONTROL ?

Before proceeding, it is necessary to address the question: - "Why use angular control?".

Even without recourse to detailed analysis it is possible to visualize cases where application of angular control could be beneficial.

Figure 2 shows typical mode shapes for a flexibly-mounted uniform shaft having both stiff and soft supports. In Figure 2a the mode shapes are presented in the conventional fashion, i.e.. in the form of shaft *lateral* displacement. Figure 2b presents similar information but using shaft *angular* displacement (slope). In this way the points of occurrence of nodes and anti-nodes, important when considering control effectiveness, can be readily compared for both control cases.

If control is considered to be implemented at the supports, it is clear that for large support stiffness values the existence of *lateral* nodes close to the support would lead to reduced radial control effectiveness. In contrast, the emergence of *angular* antinodes in this region would greatly enhance the angular control capability.

More generally, the fact that radial and angular antinodes do not necessarily occur at the same location (Fig. 2) indicates that by considering angular control the machine designer is presented with options not previously accessible.

RADIAL VERSUS ANGULAR CONTROL

The effectiveness of angular control is most easily assessed by examining the relative performance of radial and angular control implementations on a representative shaft system. For the purpose of this investigation only damping control is considered.

COMPARISON APPROACH

The comparison is performed by considering the commonly adopted model of a uniform shaft on flexible supports. This approach enables us to make use of dimensionless performance parameters which assists in broadening the applicability of the results.

Figure 3 shows the shaft system under analysis. The control methods are assessed by studying

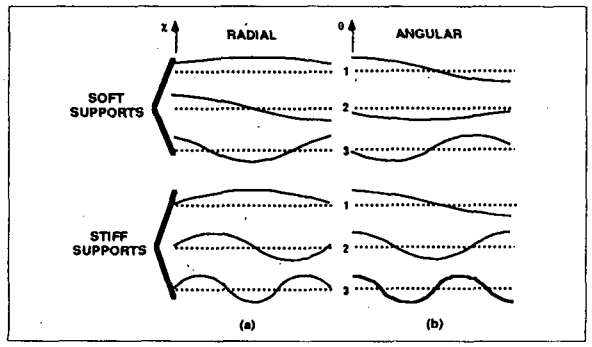

FIGURE 2. RADIAL AND ANGULAR VIBRATION MODE SHAPES

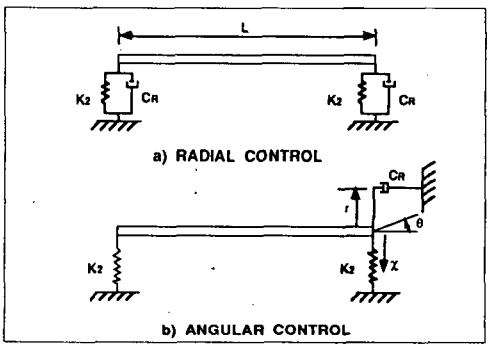

FIGURE 3. RADIAL AND ANGULAR CONTROL MODELS

the influence of the introduction of control damping at the supports.

Modal frequency and damping are determined numerically, as a function of stiffness ratio (support stiffness/shaft stiffness) K, using an eigenvalue analysis program.

To enable direct comparison of the analysis results it is assumed that equal linear damping coefficients are employed in both the radial and angular control cases. That is, referring to Figs 3, the angular damping rate C_A is given by:

$$C_A = C_r . r^2 \qquad (1)$$

The eigenvalue analysis program employed for the analysis has been constructed to utilize the damping parameter as defined in equation (1) for angular control assessment.

Control Performance Assessment

For comparison purposes use is made of the fact that in rotordynamic systems, such as the one being considered here, only minor changes in the system damped frequencies occur even when substantial damping is introduced. This results from the fact that the system eigenvectors, are relatively insensitive to damping [7]. Figure 4 illustrates this phenomenon, for the case shown in Figs 3, (with EI = 4230 Nm^2; L = 0.956m) and shows the eigenvalue locii as a function of radial support damping for stiffness ratio K = 1.0.

Investigation of the model for stiffness ratios in the region 1 - 10 showed that, generally, modal damping levels of as much as 70% of the respective optimum level (for flexural modes) could be achieved with damped-frequency changes of much less than 10%. In the case of rigid-body modes it was found that critical damping could be achieved with similarly small frequency changes.

This fact allows us to predict a linear relationship between the input control damping and the resulting modal damping, thus simplifying the comparison procedure.

Figure 5 shows the results of a regression analysis performed using the data from Fig. 4, for the first and fifth vibration modes. The slope of the graph gives the change in Log Dec, of the respective mode, per unit of control damping and will thus be termed the Damping Control Rate.

This Control Rate parameter has been computed for each of the first five system vibration modes, over a range of stiffness ratio values of 0.1 to 10, for radial and angular control types.

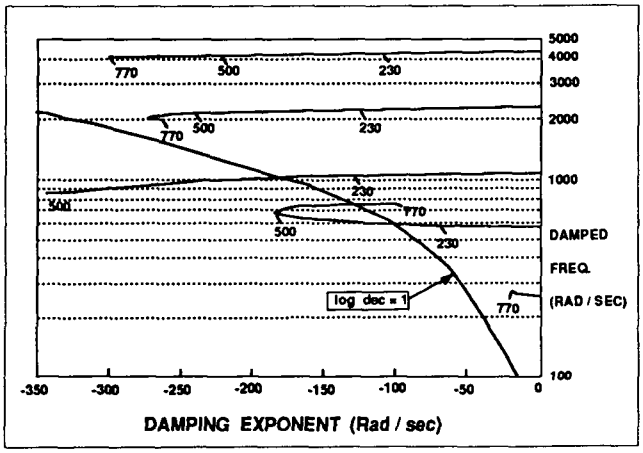

FIGURE 4. EFFECT OF RADIAL DAMPING ON EIGENVALUES (STIFFNESS RATIO K = 1.0)

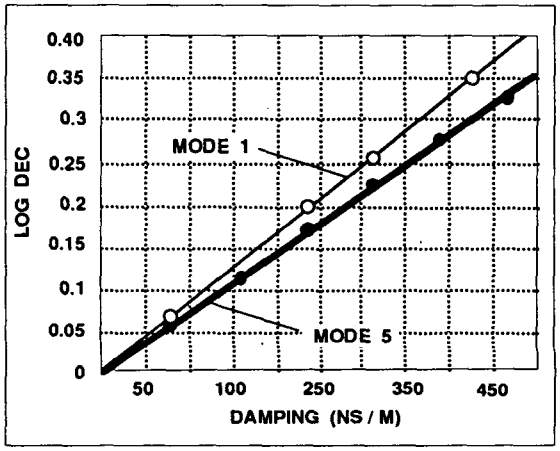

FIGURE 5. MODAL DAMPING VERSUS (RADIAL) CONTROL DAMPING; K = 1.0

The computed angular Control Rate values are subsequently modified to take account of the moment arm effect to enable direct comparison with radial Control Rates. A new dimensionless parameter defining the efficiency of angular (damping) control relative to radial (damping) control can be computed, viz : -

$$\text{Damping Control Ratio} = \frac{\text{Modified Angular Control Rate}}{\text{Radial Control Rate}}$$

Therefore, when both types of control are equally effective the Damping Control Ratio is equal to unity. A value greater than unity indicates the superiority of angular control and vice-versa.

RESULTS OF THE ANALYSIS

The effectiveness of angular control is clearly greatly dependent on the radial distance from shaft centerline to the electromagnets, i.e. the magnitude of the moment arm r.

For the purpose of this investigation this parameter is defined in terms of the ratio R = r/L. Values of R = .05, .1 and .15, felt to be acceptable in practical installations, were considered for presentation of the results. In interpreting the analysis results presented here it is important to recognize that the performance of angular control has been measured *relative* to radial control and no reference is made to absolute performance.

Figure 6 shows the control-ratio plots for the first five system modes, as a function of stiffness ratio, K. The first mode control-ratio (Fig. 6a) is seen to increase monotonically as the stiffness ratio increases, i.e. as the shaft becomes relatively more flexible angular damping performance improves substantially. For stiffness ratios in the range 2 to 4, depending on the value of the radius parameter R, both radial and angular control are observed to be equally effective. At higher stiffness ratios radial nodes are in close proximity with the supports and the superiority of angular control is evident.

In contrast, when the shaft is relatively rigid (K = 0.1 to 1.) control of the first two (rigid-body) modes deteriorates when using the angular approach. In the case of the second mode (Fig. 6b) this situation is not improved until the stiffness ratio is increased significantly (K > 4).

The control-ratio plots for modes 2 and 3 exhibit regions where angular control becomes totally ineffective. This is due to the emergence of angular nodes close to the support at stiffness ratios of 2 and 10 for the second and third modes, respectively.

The control-ratio plots for modes 3, 4 and 5 (Figs 6c to 6e) are all very similar from the point of view that effective angular control can be achieved over a wide stiffness-ratio range. In the case of the third mode the control-ratio varies from 0.2 to 0.5 over the stiffness-ratio range K = .1 to 4 (for R = 0.15). The minimum control-ratios for the fourth and fifth modes, for the same conditions, are found to be 1 and 2., respectively. More specifically, at low stiffness ratios (K < 1) modes 3, 4 and 5 become the shaft flexural modes and the influence of angular control is even more pronounced.

This has important implications when considering present-day magnetic bearings. AMB's operate with low stiffness (generally K≈1) so that rigid body modes are well damped in such a case. However, control of the flexural modes can be more difficult and the designer must ensure the absence of radial nodes. The ability of angular control to significantly influence the flexural modes in these circumstances could therefore greatly assist the designer.

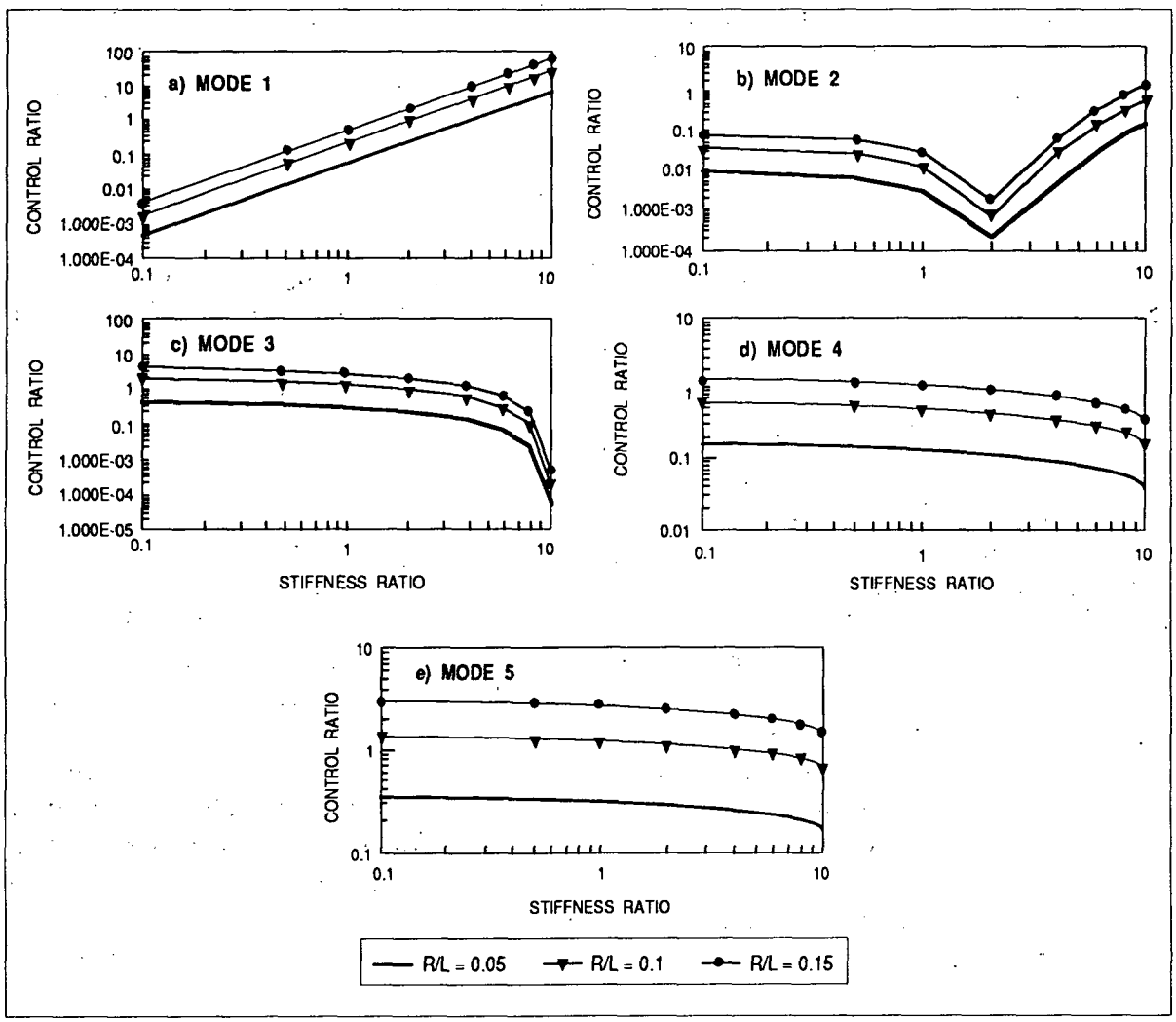

FIGURE 6. CONTROL-RATIO PLOTS

EXAMPLE

Chen [8] recently analyzed a full-scale vertical pump rotor which uses magnetic bearings. This case is selected for further analysis due to it's practical relevance and because of the availability of modelling data. The pump is designed to operate at 1800 rpm. Figure 7 shows the lumped-parameter rotor model employed for the analysis. Tables I and II summarize the rotor and radial AMB parameters as estimated from ref. [8]. Table III provides the computed damped frequency information for the following three cases,

CASE A - Radial AMB's used as per ref [8].

CASE B - Angular Damping, C_A = 2000 Nms/rad, implemented at bearings 1 and 2.

CASE C - Angular Damping, C_A = 2000 Nms/rad, implemented at the impeller.

In cases B and C the appropriate radial AMB stiffness values are used, but radial damping has been removed.

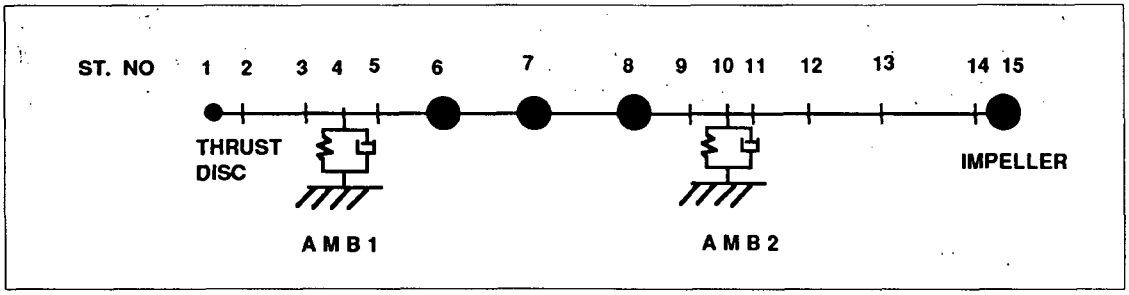

FIGURE 7. MODEL OF PUMP ROTOR (REF [8]).

Table I. Estimated Pump Model Parameters (ref [8])

Stat. No.	Sect. Length (m)	Stiff OD (m)	Ext. Mass (kg)	Inertia I_T(kgm²)	Inertia I_p(kgm²)
1	0.05	0.1	12.35	0.077	0.154
2	0.1125	0.1125	12.35	0.077	0.154
3	0.05	0.1125	2.13	0.0047	0.0094
4	0.05	0.1125	4.25	0.0094	0.0187
5	0.1	0.155	2.13	0.0047	0.0094
6	0.2125	0.155	33.85	0.211	0.422
7	0.2125	0.155	67.70	0.422	0.844
8	0.1	0.155	33.85	0.211	0.422
9	0.05	0.1125	2.13	0.0047	0.0094
10	0.05	0.1125	4.25	0.0094	0.0187
11	0.1125	0.1125	2.13	0.0047	0.0094
12	0.2375	0.0875	0	0	0
13	0.2375	0.0875	0	0	0
14	0.075	0.0875	32.13	0.301	0.602
15	0	0	32.13	0.301	0.602

Table II. Estimated AMB Parameters (ref [8])

Frequency (Hz)	AMB Stiffness (N/m)	AMB Damping (Ns/m)
20	1.09 E + 7	2.79 E + 4
47	1.50 E + 7	2.55 E + 4
99	2.07 E + 7	1.39 E + 4
334	2.69 E + 7	1.84 E + 3

Table III. Predicted Damped Frequencies for Pump Model

Mode No.	Case A		Case B		Case C	
	damped freq.(cpm)	log dec	damped freq.(cpm)	log dec	damped freq.(cpm)	log dec
1 (forw.)	1320	0.951	1319	0.465	1330	0.627
(back.)	1363	0.941	1373	0.481	1386	0.633
2 (forw.)	2764	1.661	2890	0.097	2916	0.069
(back.)	2782	1.648	2912	0.102	2934	0.070
3 (forw.)	6786	0.439	6613	0.451	7098	1.307
(back.)	7177	0.435	7053	0.454	7569	1.040
4 (forw.)	19623	4.1E-4	17924	0.391	14811	4.820
(back.)	21228	2.1E-4	19414	0.430	18774	5.180

DISCUSSION OF RESULTS

Referring to Table III computed modal frequency and damping values for case A agree fairly well with those presented by Chen [8]. The fourth shaft modes (forward and backward) are observed to be extremely lightly damped, in line with Chen's findings. The first three vibration modes are adequately damped. Of these modes the third (backward) mode exhibits least damping, having a logarithmic decrement of 0.44 which corresponds to an amplification factor (AF) of 7.2.

In contrast, when angular damping is introduced at both bearings (Case B) it is seen that all modes, other than the second, are adequately damped. Available damping for the first mode is about half that observed in Case A whilst third-mode damping levels have increased slightly. Most noticeable is the dramatic improvement in stability of the fourth mode (Log dec = .39 ; AF = 8.0), which was previously effectively undamped.

Angular damping is seen to be even more effective when applied at the impeller (Case C) - although in practice operation of the electromagnets in the process fluid and/or provision for additional sealing may rule out this option. The first mode is suitably damped whilst the third and fourth modes are now well-damped, having amplification factors of 2.5 (Log dec = 1.3) and 0.8 (Log dec = 4.8), respectively. The second mode remains very lightly damped.

It is worth noting that, although not shown here, the addition of angular damping in this case leads to significant improvement in the damping of vibration modes higher than the fourth.

The results here underline the differing modal-control influences of the radial and angular approaches.

ELECTROMAGNET REQUIREMENTS

Continuing with the above example, assume that angular control is implemented as shown in Fig. 8. Only derivative control is employed and linearization of the magnet current-force relationship might be achieved by incorporating square-root circuitry [9]. An ideal control circuit is considered, i.e.. it is assumed that none of the control components exhibit time-delays. The angular damping rate can be calculated from,

$$C_A = K_i . C_v . r . d \qquad (2)$$

Also, each electromagnet exerts a moment of amplitude M where,

$$M = F. r = K_i . i . r$$

Assuming this to be a damping moment the current i is given by,

$$i = \frac{\omega . C_A . \theta}{K_i . r} \qquad (3)$$

For small shaft angular displacements,

$$K_i = \frac{\mu_0 . A . N^2}{G} \qquad (4)$$

Equations (2), (3) and (4) were used to obtain an estimate of magnet and control parameters based on the angular damping requirement of 2000 Nms/rad. For peak current calculation it was assumed that shaft displacement at the sensors would be limited to 76 microns (3 mils) peak to peak at 1800 cyc/min.

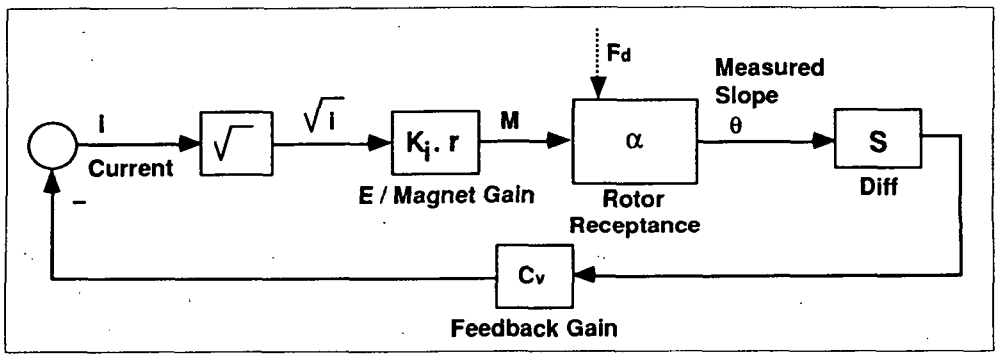

FIGURE 8. ANGULAR CONTROL CIRCUIT

The displacement transducers are assumed to have a sensitivity of 7.9 mV/micron (200 mV/mil). The estimated parameters are as follows,

Magnet leg cross-section = .045m x .045m
N = 150 ; G = 0.3×10^{-3} m ; d = 0.2m
r = 0.1m ; K_i = 636 N/amp ; C_v = 157 amp/m/sec
Peak magnet current = 1.5 amps

The maximum flux density is computed as 0.95 Tesla which leaves little margin against saturation, but this is felt to be acceptable for the present analysis given some of the assumptions involved. Note that all magnet current is used for control purposes since no steady current exists. This should result in better utilization of the magnet core but increased eddy-current loss effects would need to be considered.

Comparison of the control circuit parameters with those of Chen [8] shows that an increase in feedback gain would be required, in the case of angular control, due to the nature of the slope measurement. The computed feedback gain of 157 amp/m/s is equivalent to a gain of 330,000 amp/m at 20,000 cyc/min which is approximately ten times that used by Chen.

The magnet dimensions are fairly large but not excessive. However, further investigation of magnet heat-loss and control bandwidth-limitations will be required before specific conclusions can be drawn.

It should be stressed that no attempt has been made to optimize the application of angular control in this case and the above calculations are intended only to enable a preliminary assessment of the proposed control strategy.

Even so, the results at this stage indicate that practical implementation of angular control using electromagnets is a feasible proposition.

CONCLUSIONS

The concept of angular control has been introduced and assessed analytically on a simple flexible rotor system and on a full-scale pump rotor. Effective angular damping control of multi mode systems has been demonstrated.

The ability of angular control to significantly influence shaft flexural modes, particularly on systems having low stiffness ratios, is compatible with the effective rigid-body control characteristics of present-day active magnetic bearings. It seems logical, therefore, to consider a combined radial/angular approach. In this way the rotordynamicist should have greater freedom in the selection of system parameters.

Although an attempt has been made herein to generalize the results it is clear that the merits of angular control could only be properly judged on a case-by-case basis.

Analysis of a pump rotor highlighted the ability of radial and angular control methods to influence the same vibration modes to differing extents. This underlines the complementary nature of the control methods.

Implementation of angular damping control on a full-scale rotor using electromagnets looks to be possible. However, more detailed studies on the control-circuitry and electromagnet requirements will be required.

Nomenclature

A = Magnet Pole Face, per pole (m^2)	K = Stiffness Ratio = K_2/K_1
C_A = Angular Damping Rate (Nms/Rad)	Ki = Electromagnet Gain (N/amp)
C_r = Radial Damping Rate (Ns/m)	L = Shaft Span (m)
C_v = Feedback Gain (Amp/m/sec)	M = Electromagnet Moment (Nm)
d = Distance Between Displacement Sensors (m)	N = Magnet Coil Turns per Pole
E = Young's Modulus of Elasticity (N/m^2)	r = Magnet Moment Arm (m)
F = Electromagnet Force (N)	R = r/L
F_d = Effective External Disturbance Force (Nm)	x = Radial Displacement (m)
G = Magnet Air Gap (m)	α = Rotor System Receptance (m/Nm)
i = Current (Amps)	μ_o = Permeability of Air Gap = $4\pi \times 10^{-7}$ (Web/am)
I = Second Moment of Arae (m^4)	θ = Shaft Slope at Electromagnet (Rad)
K_1 = Shaft Stiffness = $48EI/L^3$ (N/m)	ω = Vibration Frequency (Rad/sec)
K_2 = Support Stiffness (N/m)	

REFERENCES

1. Kirk, R.G., J.F. Hustak, K.A. Schoeneck, 1988. "Analysis and Test Results of Two Centrifugal Compressors Using Active Magnetic Bearings". Conf on Vibn of Rotating Machinery, Paper No C278/88.

2. Cataford, G.F., R.P. Lancee, 1986. "Oil-Free Compression on a Natural Gas Pipeline". ASME Paper No 86-GT-293.

3. Lewis, D.W., R.R. Humphris, P.W. Thomas, 1989. "Active Magnetic Control of Oscillatory Axial Shaft Vibrations in Ship Shaft Transmission Systems - Part 2". Trib Trans, 32 (2) ; 179-188.

4. Redmond, I., R.F. Mclean, C.R. Burrows, 1985. "Vibration Control of Flexible Rotors". ASME Paper No 85-DET-127.

5. Zlotykamien, H.. 1988. "The Active Magnetic Bearing Enables Optimum Control of Machine Vibrations". Conf Vibn of Rotating Machinery, Paper No C303/88.

6. Burrows, C.R.. 1988. "Control Strategies for Use With Magnetic Bearings". Conf on Vibn of Rotating Machinery, Paper No C273/88.

7. Redmond, I.. 1985. "Vibration Reduction of Flexible Rotors". Phd Dissertation, University of Strathclyde, Glasgow, Scotland.

8. Ming Chen, H.. 1989. "Magnetic Bearings and Flexible Rotor Dynamics". Trib Trans, 32 (1) : 9-15.

9. Lim, T.M.. 1987. "The Development of a Simple Magnetic Bearing for Vibration Control". Phd Dissertation, University of Strathclyde, Glasgow, Scotland.